Available online at www.sciencedirect.com
SCIENCE DIRECT®
Journal of Sound and Vibration 287 (2005) 101–115
JOURNAL OF SOUND AND VIBRATION
www.elsevier.com/locate/jsvi

Dynamical analysis of a two-parameter family for a vibro-impact system in resonance cases

Wangcai Ding[a,*], Jianhua Xie[b]

[a]*School of Mechanical Engineering, Lanzhou Jiaotong University, Lanzhou 730070, People's Republic of China*
[b]*Department of Applied Mechanics and Engineering, Southwest Jiaotong University, Chengdu 610031, People's Republic of China*

Received 29 April 2004; received in revised form 13 September 2004; accepted 27 October 2004
Available online 22 December 2004

Abstract

Dynamics of a two-degree-of-freedom vibro-impact system in resonance is considered. The dynamical model and Poincaré maps are established. When a pair of complex conjugate eigenvalues of the Jacobian matrix cross the unit circle and satisfy the resonant condition $\lambda_0^4 = 1$ or $\lambda_0^3 = 1$, the four-dimensional map is reduced to a two-dimensional one by the center manifold theorem, and the reduced map is put into its normal form by the method of normal form. The two-parameter unfoldings of local dynamical behavior studied in this paper develop the results of one-parameter family analysis. The Hopf and subharmonic bifurcation conditions of period n–1 motion are given. The numerical simulation method confirms the theoretical analysis. It is shown that there exists an invariant torus via Hopf bifurcation and period 4–4 motions via subharmonic bifurcation as two controlling parameters varying near the critical point for the resonance $\lambda_0^4 = 1$, and that there exists an invariant circle and unstable fixed points of order 3 bifurcating from the fixed point, and the system leads eventually to chaos in the resonance $\lambda_0^3 = 1$.

1. Introduction

Vibro-impact systems are often encountered in practice, for instance in the models of hammer-like devices, rotor-casing dynamical systems, collisions of solids, ships moored at dockside, etc.

*Corresponding author.
E-mail address: dingdd@163.com (W. Ding).

0022-460X/$ - see front matter © 2004 Elsevier Ltd. All rights reserved.
doi:10.1016/j.jsv.2004.10.035

Impacts give rise to nonlinearity and discontinuity so that the vibro-impact system can exhibit rich and complicated dynamic behavior and it is a good testing benchmark for nonlinear theories [1–10]. During the past decades, nonsmooth dynamics of mechanical systems with impacts have become the subject of several investigations, and many new methods have been advanced in research of vibro-impacts. Holmes et al. [1] found a Smale horseshoe map in a mathematical model for the bouncing ball. The classical pattern of period doubling bifurcation cascade was observed numerically by Thompson [2], Shaw and Holmes [3]. Whiston [4], Ivanov [5] and Nordmark [6] studied the singularities of maps derived from vibro-impact systems and proved that such systems could undergo "grazing bifurcation" and lead to chaotic behavior. Recently, a few researchers began to focus attention on the phenomena of Hopf bifurcations of the vibro-impact systems and studied quasi-periodic or chaotic motion [7–9]. Xie [8] and Wen [9] investigated codimension-two bifurcations corresponding to double eigenvalue -1. Wen et al. [10] analyzed nontypical route to chaos via period-doubling bifurcation and quasi-periodic bifurcation.

Iooss [11] studied the subharmonic bifurcation of one-parameter family in resonant cases ($\lambda_0^4 = 1$ or $\lambda_0^3 = 1$) for maps in $\mathbf{R}^2$ and presented the conditions of subharmonic bifurcation. Chenciner et al. [12] investigated tori bifurcations of various dimensions for high-dimensional maps. Yieh-Hei Wan [13] considered the one-parameter family diffeomorphism and obtained the conditions of Hopf bifurcation in the resonance $\lambda_0^4 = 1$. Arnold [14,15] studied bifurcations of periodic solutions for differential equation in resonant cases, and obtained topological classifications of phase portraits for two-parameter families. Luo et al. [16] gave one-parameter family analysis of bifurcations of period n–1 motions in two resonant cases for a two-degree-of-freedom (2-dof) vibro-impact system.

In this paper, we investigate the two-parameter dynamics in two resonant cases $\lambda_0^3 = 1$ and $\lambda_0^4 = 1$ for the same model of Ref. [16]. The two-parameter unfoldings of local dynamical behavior are studied by theoretical methods, which develop the results obtained by one-parameter family model. The conditions of Hopf bifurcation and subharmonic bifurcation from period n–1 motion are put forward. In Section 2, the dynamical model and Poincaré maps are established, and then period n–1 motion and its stability are studied by analytical methods. In 3.1, when a pair of complex conjugate eigenvalues of the Jacobian matrix cross the unit circle and satisfy the condition of the resonance $\lambda_0^4 = 1$, the four-dimensional map was reduced to a two-dimensional one by the center manifold method, and the reduced map was transformed into its normal form by choosing a new base. We obtained the conditions which determined whether the fixed point would bifurcate to an invariant or to cycles of period 4. Furthermore, we recall the divisions of parameter A-plane which are investigated by Arnold [14], Berezovskaia [17] and Krauskopf [18,19]. In 3.2, we introduce the Arnold method in Refs. [14,15] to investigate the resonance $\lambda_0^3 = 1$. The partition of parameter plane and phase portraits are obtained. Numerical simulation results in Section 4 verified the theoretical analysis of Section 3. The schematic diagram of division of the parameter plane is drawn and there are topologically different phase portraits for every region. It was shown that there existed an invariant torus via Hopf (Neimark–Sacker) bifurcation and period 4–4 motions via subharmonic bifurcation as two controlling parameters varying near the critical point for the resonance $\lambda_0^4 = 1$. For the resonance $\lambda_0^3 = 1$, there might exist a stable invariant circle and an unstable cycle of period 3 bifurcating from the fixed point, and then the system leads eventually to chaos.

2. The mechanical model and periodic motion of the vibro-impact system

The model for a 2-dof vibro-impact system is shown in Fig. 1. The masses M_1 and M_2 are connected to linear springs with stiffness K_1 and K_2. Proportional damping is assumed. The mass M_1 impacts against a rigid surface W when its displacement X_1 equals the gap B. The impact is described by coefficient of restitution R.

Between impacts, the governing equations are written in a nondimensional form [7]

$$\begin{bmatrix} 1 & 0 \\ 0 & v_m \end{bmatrix} \begin{Bmatrix} \ddot{x}_1 \\ \ddot{x}_2 \end{Bmatrix} + \begin{bmatrix} 2\zeta & -2\zeta \\ -2\zeta & 2\zeta(1+v_s) \end{bmatrix} \begin{Bmatrix} \dot{x}_1 \\ \dot{x}_2 \end{Bmatrix} + \begin{bmatrix} 1 & -1 \\ -1 & 1+v_k \end{bmatrix} \begin{Bmatrix} x_1 \\ x_2 \end{Bmatrix} = \begin{Bmatrix} 1-f_{20} \\ f_{20} \end{Bmatrix} \sin(\omega t + \tau) \quad (x_1 < b) \tag{1}$$

and the impact equation of mass M_1 is

$$\dot{x}_{1+} = -R\dot{x}_{1-} \quad (x_1 = b), \tag{2}$$

where a dot denotes differentiation with respect to the nondimensional time t, $\dot{x}_{1+}$ and $\dot{x}_{1-}$ represent, respectively, the departure and approach velocities of M_1 at the instant of impact, and the nondimensional quantities are of the forms

$$v_m = \frac{M_2}{M_1}, \quad v_k = \frac{K_2}{K_1}, \quad v_s = \frac{C_2}{C_1} = v_k, \quad f_{20} = \frac{P_2}{P_1 + P_2}, \quad \zeta = \frac{C_1}{2\sqrt{K_1 M_1}},$$
$$\omega = \Omega\sqrt{\frac{M_1}{K_1}}, \quad t = T\sqrt{\frac{K_1}{M_1}}, \quad b = \frac{BK_1}{P_1 + P_2}, \quad x_i = \frac{X_i K_1}{P_1 + P_2} \tag{3}$$

Letting ψ represent the canonical model matrix of Eq. (1) and taking it as a transition matrix, and under the change of variables $X = \psi Z$, Eq. (1) becomes

$$I\ddot{Z} + C\dot{Z} + \Lambda Z = \tilde{F}\sin(\omega t + \tau), \tag{4}$$

where $X = (x_1, x_2)^{\mathrm{T}}$, $Z = (z_1, z_2)^{\mathrm{T}}$, I is a 2×2 identity matrix, $C = 2\zeta\Lambda = \mathrm{diag}[2\zeta\omega_1^2, 2\zeta\omega_2^2]$, $\Lambda = \mathrm{diag}[\omega_1^2, \omega_2^2]$, $\tilde{F} = (\tilde{f}_1, \tilde{f}_2)^{\mathrm{T}} = \psi^{\mathrm{T}} f$, $f = (1 - f_{20}, f_{20})^{\mathrm{T}}$, and ω_1, ω_2 are the eigenfrequencies of the

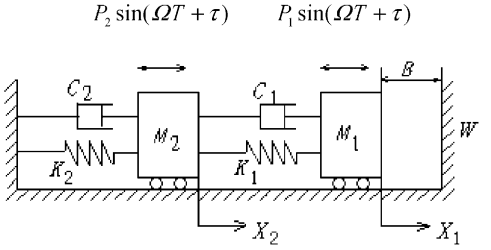

Fig. 1. The model of 2-dof vibro-impact system.

system. The general solutions of Eq. (1) are

$$x_i = \sum_{j=1}^{2} \psi_{ij}(\mathrm{e}^{-\eta_j t}(a_j \cos \omega_{dj} t + b_j \sin \omega_{dj} t) + A_j \sin(\omega t + \tau) + B_j \cos(\omega t + \tau)), \tag{5}$$

$$\dot{x}_i = \sum_{j=1}^{2} \psi_{ij}(\mathrm{e}^{-\eta_j t}((b_j \omega_{dj} - \eta_j a_j) \cos \omega_{dj} t - (\eta_j b_j + a_j \omega_{dj}) \sin \omega_{dj} t) + A_j \omega \cos(\omega t + \tau) - B_j \omega \sin(\omega t + \tau)) \quad (i = 1, 2), \tag{6}$$

where ψ_{ij} are the elements of the canonical modal matrix ψ, $\eta_j = \zeta \omega_j^2$, $\omega_{dj} = \sqrt{\omega_j^2 - \eta_j^2}$, a_j and b_j are the constants of integration which are determined by the initial condition and parameters of the system, A_j and B_j are the amplitude parameters taking the form

$$A_j = \frac{\omega_{nj}^2 - \omega^2}{(\omega_{nj}^2 - \omega^2)^2 + (2\eta_j \omega)^2} \tilde{f}_j, \tag{7}$$

$$B_j = \frac{-2\eta_j \omega}{(\omega_{nj}^2 - \omega^2)^2 + (2\eta_j \omega)^2} \tilde{f}_j. \tag{8}$$

Letting $\theta = \omega t$, we choose a Poincaré section $\sigma = \{(x_1, \dot{x}_{1+}, x_2, \dot{x}_{2+}, \theta) \in \mathbf{R}^4 \times \mathbf{S}^1, x_1 = b\}$. Suppose that a period n–1 motion (in each interval of time $2n\pi/\Omega$, a single impact occurs) starts at the point $X_0 = (\dot{x}_{10+}, x_{20}, \dot{x}_{20+}, \tau_0)$ on σ; then using Eqs. (5) and (6), we can obtain X_0 as functions of the system parameters [7]. After choosing X_0 as the origin of σ, we establish the Poincaré map associated with the period n–1 motion

$$y' = f_v(y) = f(y, v), \quad f(0, v) = 0, \tag{9}$$

where

$$y = (y_1, y_2, y_3, y_4)^{\mathrm{T}} = (\dot{x}_1 - \dot{x}_{10+}, x_2 - x_{20}, \dot{x}_2 - \dot{x}_{20+}, (\tau - \tau_0) \bmod 2n\pi)^{\mathrm{T}} \in \mathbf{R}^4$$

is the perturbed vector of the period n–1 motion in the hyperplane σ, $v = (v_1, v_2)^{\mathrm{T}} \in \mathbf{R}^2$ is the control parameter vector and v_c is the critical value of v.

Jacobi matrix of the Poincaré map (9) is

$$\mathrm{D}f(0, v) = \partial f(y, v)/\partial y|_{(0,v)}. \tag{10}$$

All entries of $\mathrm{D}f(0, v)$ were represented as functions of the parameters; high-order terms of $f(y, v_c)$ could be calculated according to the implicit theorem [7]. If all eigenvalues of $\mathrm{D}f(0, v)$ lie inside of the unit circle, the fixed point X_0 is stable, so is the period n–1 motion. If some eigenvalues penetrate the boundary of the unit circle at v_c, the fixed point X_0 loses its stability, and so does the period n–1 motion. In this case, bifurcation occurs. The type of bifurcation depends not only on the degeneracy of $\mathrm{D}f(0, v_c)$ but also on high-order terms of f_v. We will study Hopf and subharmonic bifurcations in the resonant cases $\lambda_0^4 = 1$ and $\lambda_0^3 = 1$.

3. Dynamical behavior of vibro-impact system in resonance cases

3.1. The resonance $\lambda_0^4 = 1$

Let us continue to analyze the Poincaré map (9). Suppose that in some neighborhood of a critical value $v = v_c$, $Df(0, v)$ satisfies the following assumptions:

(H1) $Df(0, v_c)$ has a pair of complex-conjugate eigenvalues $\lambda_1 = \lambda_1(v_c)$, $\lambda_2 = \bar{\lambda}_1(v_c)$ on the unit circle ($|\lambda_1(v_c)| = 1$), and the other eigenvalues $\lambda_i(v_c)$ ($i = 3, 4$) stay inside the unit circle, i.e. $|\lambda_i(v_c)| < 1$;

(H2) $\frac{\partial\lambda_1(v)}{\partial v_1}|_{v=v_c}$ and $\frac{\partial\lambda_1(v)}{\partial v_2}|_{v=v_c} \neq 0$, which is the transversal condition for the two-parameter family of Eq. (9);

(H3) $\lambda_1^4(v_c) = 1$, $\lambda_1(v_c) \neq \pm 1$.

Let

$$p(\lambda) = \lambda^4 + a_3\lambda^3 + a_2\lambda^2 + a_1\lambda + a_0 = 0 \tag{11}$$

be the characteristic equation for matrix $Df(0, v)$. Then we have following lemma,

Lemma. *The roots of Eq.* (11) *satisfy* (H1) *if and only if*

(a1) $|a_0| < 1$;

(a2) $|a_1 + a_3| < 1 + a_0 + a_2$;

(a3) $a_2(1 - a_0) + a_0(1 - a_0^2) + a_3(a_0a_3 - a_1) > 0$; *and*

(a4) $a_2(1 - a_0) + a_0(1 - a_0^2) + a_3(a_0a_3 - a_1) = a_0a_2(1 - a_0) + (1 - a_0^2) + a_1(a_0a_3 - a_1) = 0$, *where* $a_i \in \mathbf{R}$ ($i = 0, 1, 2, 3$) *is dependent upon parameters of the system.*

Let r_i denote the eigenvectors of $Df(0, v)$ corresponding to $\lambda_i(v)$ ($i = 1, 2, 3, 4$). If r_3 and r_4 are a complex-conjugate pair of eigenvectors, then let eigenmatrix $P = (\mathrm{Re}\, r_1, -\mathrm{Im}\, r_1, \mathrm{Re}\, r_3, -\mathrm{Im}\, r_3)$, otherwise, let $P = (\mathrm{Re}\, r_1, -\mathrm{Im}\, r_1, r_3, r_4)$. By changing variables

$$y = PY, \quad \mu = [\mu_1, \mu_2]^{\mathrm{T}} = v - v_c \tag{12}$$

map (9) becomes

$$Y' = F(Y, \mu), \tag{13}$$

where $Y = (y_1, y_2, y_3, y_4)^{\mathrm{T}}$, and $DF(0, \mu)$ takes the form

$$DF(0, \mu) = \begin{bmatrix} \alpha & -\omega & & \\ \omega & \alpha & & \\ & & & D \end{bmatrix} \tag{14}$$

with $\alpha = \mathrm{Re}\,\lambda_1(v_c + \mu)$, $\omega = \mathrm{Im}\,\lambda_1(v_c + \mu)$, and D is a real 2×2 matrix with eigenvalues $\lambda_3(\mu)$ and $\lambda_4(\mu)$.

For map (13), there exists a center manifold [20] $W(z,\bar{z};\mu)$ on which map (13) can be reduced to a two-dimensional map $\Phi_\mu : \mathbf{C} \to \mathbf{C}$, or

$$z' = \lambda(\mu)z + \sum_{i+j=2}^{3} g_{ij}(\mu)\,\frac{z^i\bar{z}^j}{i!j!} + O(|z|^4) \tag{15}$$

with

$$\lambda(\mu) = \lambda_0(1 + \mu_1\tilde{\lambda}_1 + \mu_2\tilde{\lambda}_2 + O(\|\mu\|^2)), \tag{16}$$

where $\lambda(\mu) = \lambda_1(v_c + \mu)$, $\lambda_0 = \lambda(0) = \mathrm{i}$, $\tilde{\lambda}_1 = -\mathrm{i}\partial\lambda(0)/\partial v_1$, $\tilde{\lambda}_2 = -\mathrm{i}\partial\lambda(0)/\partial v_2$, $z = y_1 + \mathrm{i}y_2$, $\bar{z} = y_1 + \mathrm{i}y_2$, and $g_{ij}(\mu)$ $(i+j=2,3)$ were given in Ref. [7].

According to the normal form theory [11], there exists smooth μ-dependent change of coordinate which puts map (15) into its normal form

$$\Phi_\mu(z,\bar{z}) = \lambda(\mu)z + \alpha(\mu)z^2\bar{z} + \beta(\mu)\bar{z}^3 + O(|z|^5), \tag{17}$$

where $\alpha(0)$ and $\beta(0)$ take forms

$$\alpha(0) = \frac{g_{21}}{2} + \frac{|g_{02}|^2}{2(\lambda_0^2 - \bar{\lambda}_0)} + \frac{|g_{11}|^2}{1-\bar{\lambda}_0} + \frac{g_{11}g_{20}(1-2\lambda_0)}{2(\lambda_0^2-\lambda_0)}, \tag{18}$$

$$\beta(0) = \frac{g_{03}}{6} + \frac{g_{02}(g_{11}+g_{20})}{2(\bar{\lambda}_0^2 - \lambda_0)}, \tag{19}$$

where $g_{ij} = g_{ij}(0)\,(i+j=3)$.

Define a_1 and a_2 as

$$a_1 = \frac{\alpha(0)}{\lambda_0}, \quad a_2 = \frac{\beta(0)}{\lambda_0}. \tag{20}$$

Suppose that μ varies in some neighborhood of $[0,0]^{\mathrm{T}}$, we have

$$z' = \Phi_\mu(z,\bar{z}) = \lambda(\mu)(z + a_1z^2\bar{z} + a_2\bar{z}^3) + O(|z|^5). \tag{21}$$

Let us put, Eq. (21) in polar coordinates: $z = r\mathrm{e}^{\mathrm{i}\theta}$. Then the new form of the map is

$$\begin{aligned} r' &= |\lambda|r[1 + a_{1r}r^2 + (a_{2r}\cos 4\theta + a_{2i}\sin 4\theta)r^2] + O(r^5),\\ \theta' &= \theta + \varphi + a_{1i}r^2 + (a_{2i}\cos 4\theta - a_{2r}\sin 4\theta)r^2] + O(r^4), \end{aligned} \tag{22}$$

where $a_{1r} = \mathrm{Re}(a_1)$, $a_{1i} = \mathrm{Im}(a_1)$, $a_{2r} = \mathrm{Re}(a_2)$, $a_{2i} = \mathrm{Im}(a_2)$, $\varphi = \arg\lambda$.

We define the new parameters ξ_1, ξ_2 by

$$\xi_1 = |\lambda| - 1, \quad \xi_2 = \varphi - \varphi_0 \tag{23}$$

with $\varphi_0 = \arg\lambda_0$. Map (22) is changed into $F_\xi : (r,\theta) \to (r',\theta')$, or

$$F_\xi : \begin{cases} r' = (1+\xi_1)r[1 + a_{1r}r^2 + (a_{2r}\cos 4\theta + a_{2i}\sin 4\theta)r^2] + O(r^5),\\ \theta' = \theta + \varphi_0 + \xi_2 + a_{1i}r^2 + (a_{2i}\cos 4\theta - a_{2r}\sin 4\theta)r^2] + O(r^4). \end{cases} \tag{24}$$

Let us look for fixed points of order 4 which satisfy the equation $F_{\xi}^{4}(r,\theta)=(r,\theta)$, after neglecting the higher-order terms and noting the fact $4\varphi_0 = 0 \bmod 2\pi$, we have

$$\begin{aligned}&(1+4\xi_1)[1+4a_{1r}r^2+4(a_{2r}\cos 4\theta+a_{2i}\sin 4\theta)r^2]=1,\\&\xi_2+a_{1i}r^2+(a_{2i}\cos 4\theta-a_{2r}\sin 4\theta)r^2]=0.\end{aligned} \tag{25}$$

Eliminating r^2 from Eq. (25), we obtain

$$\frac{\xi_2}{\xi_1}=\frac{a_{1i}+a_{2i}\cos 4\theta-a_{2r}\sin 4\theta}{a_{1r}+a_{2r}\cos 4\theta+a_{2i}\sin 4\theta}. \tag{26}$$

Let $d=\xi_2/\xi_1$. When ξ_1 and ξ_2 in Eq. (26) take suitable values, we can solve θ which corresponds to the fixed point of order 4 for map (9). From Eq. (26),

$$\sin(4\theta-\beta_0)+d\cos(4\theta-\beta_0)=(a_{1i}-a_{1r}d)/|a_2|, \tag{27}$$

where $\beta_0=\arg a_2$. After dividing the equation above by $\sqrt{1+d^2}$, we get

$$\sin(4\theta-\beta_0+\gamma_0)=\frac{a_{1i}-a_{1r}d}{|a_2|\sqrt{1+d^2}}, \tag{28}$$

where $\gamma_0=\tan^{-1}d$. So we obtain the condition which guarantees the existence of fixed points of order 4, that is

$$|a_{1i}-a_{1r}d|\leqslant|a_2|\sqrt{1+d^2}. \tag{29}$$

There are two families of solutions: $\theta_k=\theta_0+k\pi/2$ and $\theta_k'=-\theta_0+k\pi/2$, $k=0,1,2,3$, where θ_0 is the minimal solution of Eq. (28), and at least one of the families is unstable [11].

Condition (29) is equivalent to

$$d_1\leqslant d\leqslant d_2, \tag{30}$$

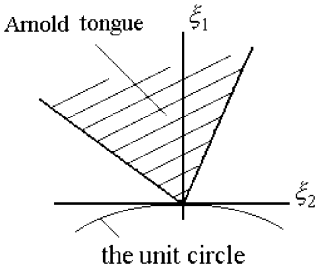

Fig. 2. Arnold tongue at $\lambda_0=$ i.

where

$$d_{1,2} = \frac{a_{1r}a_{1i}\mu|a_2|\sqrt{|a_1|^2 - |a_2|^2}}{a_{1r}^2 - |a_2|^2}. \tag{31}$$

It is obvious that we need

$$|a_2| < |a_1| \quad \text{and} \quad |a_{1r}| \neq |a_2|. \tag{32}$$

Condition (30) defines an Arnold tongue for the resonance $\lambda_0^4 = 1$ [14]. When the eigenvalue λ belongs to the Arnold tongue (see Fig. 2), two period n–4 motions occur for the vibro-impact system, and usually they have the opposite stabilities. When the parameters satisfy $d < d_1$ or $d > d_2$, Hopf bifurcation may take place and a quasi-periodic motion appears. Since $d_1 \neq -d_2$ in general, the Arnold tongue is asymmetrical with the imaginary axis.

In this case it is possible to approximate (17) by the "time-1 map" of the flow of a $\mathbf{Z}_4$-equivariant vector field. Due to its $\mathbf{Z}_4$-symmetry we obtain

$$\dot{z} = \varepsilon z + \alpha(\mu)z^2\bar{z} + \beta(\mu)\bar{z}^3 + O(|z|^5), \tag{33}$$

where $\varepsilon = \xi_1 + \mathrm{i}\xi_2$. By means of rescaling z and time [14], we have

$$\dot{z} = \varepsilon z + Az^2\bar{z} + \bar{z}^3, \tag{34}$$

where $A = \alpha(\mu)/|\beta(\mu)|$.

The bifurcation analysis of system (34) is very complicated and requires numerical techniques [18]. The bifurcation diagram depends on $A = A(0)$, so the A-plane is divided into several regions with different bifurcation diagrams in the (ξ_1, ξ_2)-plane (shown in Fig. 3). As one can see, the boundaries on the A-plane are symmetric under reflections with respect to the coordinate axes. Thus, it is sufficient to study them in one quadrant of the A-plane. The bifurcation sequences and phase portraits for every region are studied by Arnold [14], Berezovskaia [17] and Krauskopf

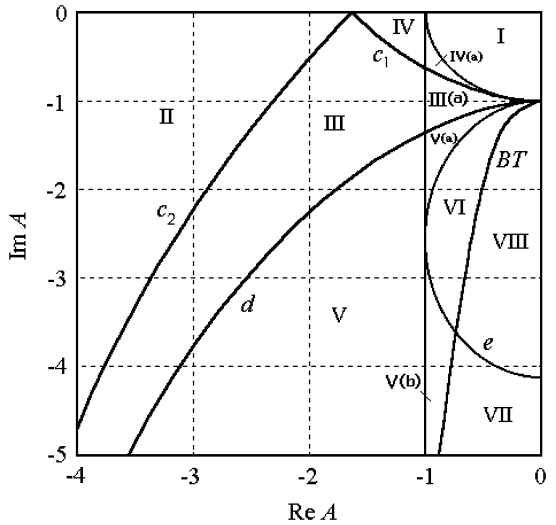

Fig. 3. Division of the A-plane into regions with different bifurcation diagrams.

[18,19], which make it possible to investigate the complicated bifurcations near the resonant point for a 2-dof vibro-impact system in the next section.

3.2. The resonance $\lambda_0^3 = 1$

Now we consider the resonance $\lambda_0^3 = 1$. Suppose that in some neighborhood of certain critical value $v = v_c$, $Df(0, v)$ satisfies the following assumptions:

(C1) $Df(0, v_c)$ has a pair of complex-conjugate eigenvalues $\lambda_1 = \lambda_1(v_c)$, $\lambda_2 = \bar{\lambda}_1(v_c)$ on the unit circle ($|\lambda_1(v_c)| = 1$); the other eigenvalues $\lambda_i(v_c)$ $(i = 3, 4)$ stay inside the unit circle, i.e. $|\lambda_i(v_c)| < 1$;

(C2) $\dfrac{\partial\lambda_1(v)}{\partial v_1}|_{v=v_c}$ and $\dfrac{\partial\lambda_1(v)}{\partial v_2}|_{v=v_c} \neq 0$, which represents the transversal condition for two-parameter family;

(C3) $\lambda_1^3(v_c) = 1$, $\lambda_1(v_c) \neq 1$.

There exists smooth μ-dependent change of coordinate which puts map (15) into its normal form

$$\Phi_\mu(z, \bar{z}) = \lambda(\mu)z + \tfrac{1}{2}g_{02}(\mu)\bar{z}^2 + \alpha(\mu)z^2\bar{z} + O(|z|^4). \tag{35}$$

Let us consider Φ_μ^3 which is the iterate map Φ_μ and, after omitting the high-order terms, we write

$$\Phi_\mu^3 = (1 + 3\mu_1\tilde{\lambda}_1 + 3\mu_2\tilde{\lambda}_2)z + \tfrac{3}{2}g_{02}\bar{\lambda}_0\bar{z}^2 + 3\alpha\bar{\lambda}_0 z^2\bar{z}. \tag{36}$$

We use $\tilde{\Phi}_\mu(z, \bar{z})$ to stand for the "time-1 map" of the following differential equation:

$$\dot{z} = \varepsilon z + \tfrac{1}{2}g_{02}\bar{z}^2 + \alpha z^2\bar{z}, \tag{37}$$

where $\varepsilon = \mu_1\tilde{\lambda}_1 + \mu_2\tilde{\lambda}_2$. It is easy to see

$$\Phi_\mu^3 \approx \tilde{\Phi}_\mu(z, \bar{z}). \tag{38}$$

Relationship (38) shows that we can use differential equation (37) to describe the dynamics of the map near the resonant point. Arnold considers in Refs. [14,15] a differential equation in C, invariant by rotations of $2\pi/3$ about the origin. The time 1 map for this equation is supposed to approximate the map Φ_μ^3 up to high-order terms. If Eq. (37) has a nontrivial equilibrium, then map (35) may possess a cycle of period 3. And furthermore, if the equilibrium of (37) undergoes a Hopf bifurcation at a certain value μ_c, and gives birth to a closed orbit, then the planar map

$$z' = \tilde{\Phi}_\mu(z, \bar{z}) \tag{39}$$

possesses an invariant circle at a certain value of parameter $\mu \approx \mu_c$ [16].

Let us define parameters by $\xi_1 = \mathrm{Re}(\varepsilon)$, $\xi_2 = \mathrm{Im}(\varepsilon)$. According to Arnold theory [14,15], the Hopf bifurcation condition for differential equation (37) is

$$\xi_1 \leqslant \rho|\mathrm{Re}(\alpha)|\xi_2^2, \tag{40}$$

where ρ denotes the radius of inertia of triangle formed from three saddle points.

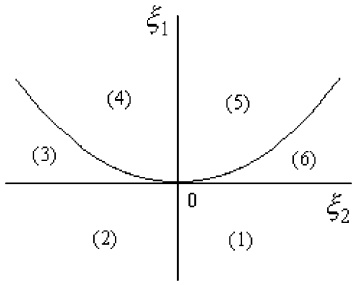

Fig. 4. The partition of parameter plane.

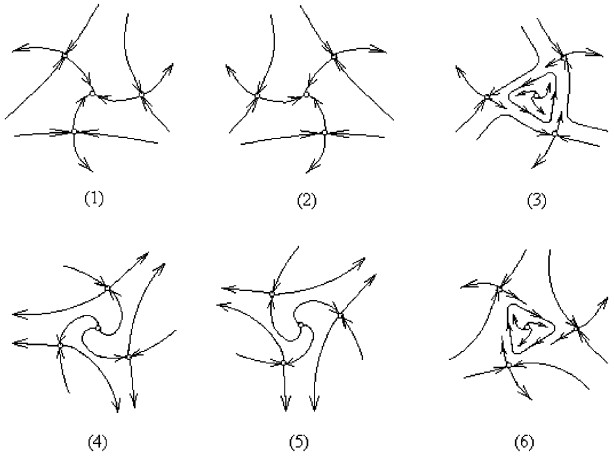

Fig. 5. The phase portraits.

It is not difficult to analyze the two-parameter unfoldings and phase portraits of Eq. (37) near the resonant point [14]. Fig. 4 shows the partition of the parameter plane, and Fig. 5 shows phase portraits corresponding to the regions of Fig. 4.

4. Numerical simulation of Hopf and subharmonic bifurcations

We use the procedure in Section 3 to compute Hopf and subharmonic bifurcations of the period n–1 motion, and then verify the results by numerical simulation. Considering the basic period 1–1 motion, we choose the first set of parameters: $v_m = 5.939971$, $v_k = 2.0$, $\zeta = 0$, $f_{20} = 0$, $R = 0.8$, and take ω and b as the control parameters, $\mu = (\mu_1, \mu_2)^{\mathrm{T}} = (\omega - \omega_c, b - b_c)^{\mathrm{T}}$. According to the theoretical analysis in the previous section and numerical computation, we obtain the bifurcation point (ω_c, b_c), the normal form coefficients and eigenvalues of $\mathrm{D}f_0(0)$ satisfying conditions (H1) and (H3), as follows:

$$\omega_{\mathrm{c}} = 0.4353907, \quad b_c = 3.1,$$

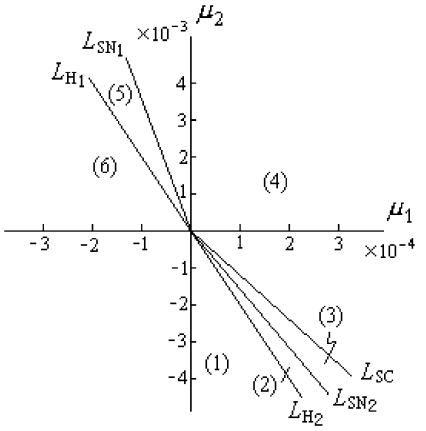

Fig. 6. Division of local bifurcation behavior under physical parameters.

$$\lambda_0, \bar{\lambda}_0 = 0.00000002 \pm 1.00000003\mathrm{i}, \quad |\lambda_0| = 1,$$

$$\lambda_{3,4} = 0.392327 \pm 697194\mathrm{i}, \quad |\lambda_3(0)| < 1.$$

$a_1 = -1.434816 - 1.029660\mathrm{i}$, $a_2 = -0.085915 + 1.022163\mathrm{i}$ and $A = -1.39877 - 1.00380\mathrm{i}$ which satisfy condition (32) and belong to region III in Fig. 3, so there exists an Arnold tongue defined by $d_1 = 0.040$, $d_2 = 2.896$. We can compute

$$\tilde{\lambda}_1 = -\mathrm{i}\,\frac{\partial\lambda(0,0)}{\partial\mu_1} = -\mathrm{i}\,\frac{\partial\lambda}{\partial\omega}(\omega_c, b_c) = 10.464 - 32.617\mathrm{i},$$

$$\tilde{\lambda}_2 = -\mathrm{i}\,\frac{\partial\lambda(0,0)}{\partial\mu_2} = -\mathrm{i}\,\frac{\partial\lambda}{\partial b}(\omega_c, b_c) = 0.524 - 1.138\mathrm{i},$$

$$\lambda(\mu) = 32.617\mu_1 + 1.138\mu_2 + (1 + 10.464\mu_1 + 0.524\mu_2)\mathrm{i} + O(\|\mu\|^2).$$

We can calculate $\xi_1(\mu)$, $\xi_2(\mu)$ and d to determine whether it is period 4–4 motions or quasi-periodic motion that bifurcates from the fixed point.

By numerical simulation, the division of the parameter plane for different behavior near the resonant point is shown sketchily in Fig. 6. In regions (1), (6) and the third quadrant in parameter plane, the fixed point is stable. When the parameters cross the line L_{H1} and L_{H2}, the Hopf (Neimark–Sacker) bifurcation occurs. When the parameters cross the line L_{SN1} and L_{SN2}, the saddle-node bifurcation occurs with the first one on and the second one outside the invariant circle. In region (3), there exists the attractive invariant circle and stable 4–4 fixed points outside the invariant circle. As the parameters pass across the line L_{SC}, the invariant circle disappears and on the line L_{SC} there is a heteroclinic loop from saddle connection. In region (4) which is bounded by the lines of saddle-node bifurcations there exist 4–4 fixed points.

A small perturbation of the fixed point $X_0 = (\dot{x}_{10+}, x_{20}, \dot{x}_{20+}, \tau_0)^{\mathrm{T}}$ is taken as an initial point of the Poincaré map (9). As μ changes near $\mu_c = (0,0)$, dynamical behavior of the vibro-impact system is displayed on the coordinate plane (τ, x_2) and on the other projected Poincaré sections of σ. Fig. 7(a) and (i) show that period 1–1 motion is stable, which correspond respectively to regions

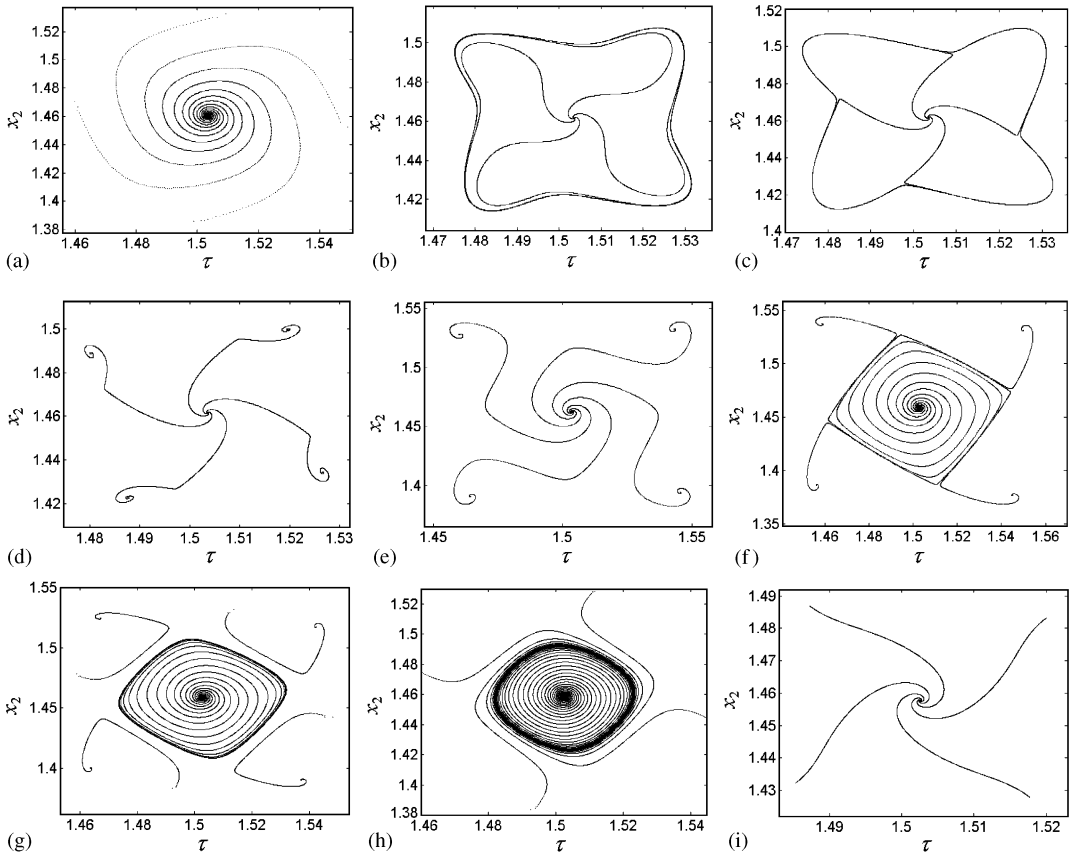

Fig. 7. The Poincaré map: (a) $\mu_1 = -0.0002$, $\mu_2 = 0.003$, stable 1–1 fixed point; (b) $\mu_1 = -0.000085$, $\mu_2 = 0.003$, attracting invariant circle or torus T^1; (c) $\mu_1 = -0.00008102$, $\mu_2 = 0.003$, attracting invariant circle or torus T^1; (d) $\mu_1 = -0.00008101$, $\mu_2 = 0.003$, stable cycle of period 4; (e) $\mu_1 = 0$, $\mu_2 = 0.003$, stable cycle of period 4; (f) $\mu_1 = 0.00024$, $\mu_2 = -0.003$, stable cycle of period 4; (g) $\mu_1 = 0.0002$, $\mu_2 = -0.003$, attracting invariant circle (or torus T^1) and stable cycle of period 4 outside the circle; (h) $\mu_1 = 0.0002$, $\mu_2 = -0.0035$, attracting invariant circle or torus T^1; (i) $\mu_1 = 0.00015$, $\mu_2 = -0.0038$, stable cycle of period 1.

(6) and (1) in Fig. 6. Fig. 7(b) shows that Hopf bifurcation of period 1–1 motion occurs and the system yields quasi-periodic motion which is an attractive invariant circle on the coordinate planes, corresponding to the region right to the Arnold tongue in Fig. 2 and region (5) in Fig. 6. By passing across the first saddle-node bifurcation (see Fig. 7(c)), subharmonic motion creates and all transitive motions settle down to a stable period 4–4 motion, Fig. 7(d), (e) and (f), corresponding to the region of the Arnold tongue in Fig. 2 and region (4) in Fig. 6. Fig. 7(f) closes to the saddle connection L_{SC} in Fig. 6. Fig. 7(g) shows that an invariant circle and period 4–4 motion coexist, corresponding to region (3) inFig. 6. Fig. 7(h) indicates that the invariant circle is the only attractor, corresponding to region (2) in Fig. 6.

Let us try another set of parameters $v_m = 1.5$, $v_k = 2.2$, $f_{20} = 0$, $R = 0.7$, $b = 1.4$. And now we take ω and ζ as the control parameters, $\mu = (\mu_1, \mu_2)^{\mathrm{T}} = (\omega - \omega_c, \zeta - \zeta_c)^{\mathrm{T}}$. As we have done to the previous set of parameters, we obtain the bifurcation point (ω_c, ζ_c), the normal form coefficients

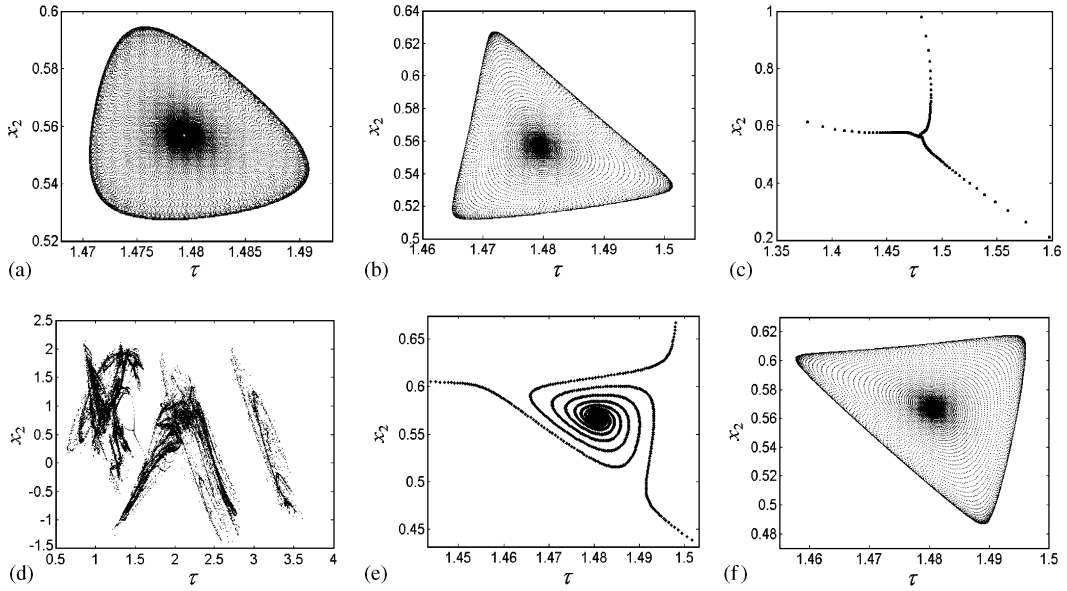

Fig. 8. The Poincaré map: (a) $\mu_1 = -0.0008$, $\mu_2 = -0.00033$, attracting invariant circle or torus T^1; (b) $\mu_1 = -0.0008$, $\mu_2 = -0.00035$, attracting invariant circle or torus T^1; (c) $\mu_1 = 0.0003$, $\mu_2 = -0.0003$, unstable period 3–3 motion (plotting for 1500 impacts); (d) $\mu_1 = 0.0003$, $\mu_2 = -0.0003$, chaos (plotting for 20,000 impacts); (e) $\mu_1 = 0.0008$, $\mu_2 = 0.0002$, unstable period 3–3 motion (plotting for 2400 impacts); (f) $\mu_1 = 0.0008$, $\mu_2 = 0.00029$, attracting invariant circles or torus T^1.

and eigenvalues of $Df_0(0)$ satisfying conditions (C1) and (C3), as follows:

$$\omega_c = 0.66473626, \quad \zeta_c = 0.00112533,$$

$$\lambda_0, \bar{\lambda}_0 = -0.50000008 \pm 0.86602546\mathrm{i}, \quad |\lambda_0| = 1,$$

$$\lambda_{3,4} = -0.182528 \pm 0.651986\mathrm{i}, \quad |\lambda_3(0)| < 1.$$

$$g_{02} = -0.098430 - 0.302762\mathrm{i}, \quad \alpha = 0.022746 - 0.028133\mathrm{i}$$

and

$$\tilde{\lambda}_1 = -\mathrm{i}\,\frac{\partial\lambda(0,0)}{\partial\mu_1} = -\mathrm{i}\,\frac{\partial\lambda}{\partial\omega}(\omega_c, \zeta_c) = 7.220 - 17.755\mathrm{i},$$

$$\tilde{\lambda}_2 = -\mathrm{i}\,\frac{\partial\lambda(0,0)}{\partial\mu_2} = -\mathrm{i}\,\frac{\partial\lambda}{\partial\zeta}(\omega_c, \zeta_c) = -17.875 - 2.091\mathrm{i},$$

$$\varepsilon(\mu) = 7.220\mu_1 - 17.875\mu_2 - (17.755\mu_1 + 2.091\mu_2)\mathrm{i} + O(\|\mu\|^2), \quad \rho = 119.6.$$

Furthermore, we can calculate $\xi_1(\mu)$ and $\xi_2(\mu)$ to determine whether or not there is a stable invariant torus between the unstable cycle of period 3 and the fixed point when the latter loses its stability.

Figs. 8(a) and (b) show that the Hopf bifurcation of period 1–1 motion occurs and the system yields quasi-periodic motion, corresponding to the region (3) in Fig. 4. Subharmonic bifurcation of period 1–1 motion occurs and the system settles down to chaos via unstable period 3–3 motion, as shown in Figs. 8(c), (d) and (e), corresponding to region (4) or (5) in Fig. 4. Fig. 8(f) shows that the Hopf bifurcation of period 1–1 motion takes place, which corresponds to region (6) in Fig. 4. When the parameter vector μ is sufficiently close to the boundary curves (the boundaries between regions (3) and (4), or between the regions (6) and (5) in Fig. 4), the invariant circle has limited smoothness and has the shape of a "triangle" (Figs. 8(b) and (f)).

5. Conclusions

In this paper, we studied the Hopf and subharmonic bifurcations in two resonance cases for a 2-dof vibro-impact system by theoretical analysis and numerical simulations. Firstly, the period n–1 motion and the four-dimensional Poincaré map of the system were established by analytical method and the stability of the periodic motion was analyzed. Secondly, by center manifold theorem and normal form methods, we reduced the four-dimensional map into its two-dimensional normal form, and obtained the analytic expressions of the normal form coefficients. Then for the resonance $\lambda_0^4 = 1$, we derived the conditions to determine whether there exists an invariant circle or fixed points of order 4 that bifurcated from the fixed point as the two control parameters changed. For the resonance $\lambda_0^3 = 1$, we introduced Arnold's method to analyze the local behavior of the vibro-impact system, and approximated the two-parameter unfolding of the reduced map by a "time-1" map of a planar autonomous differential equation, and showed that an unstable period 3–3 motion and a stable quasi-periodic motion could coexist, and might lead to chaotic motion via homoclinic bifurcations of the unstable period 3–3 motion. Finally, the results of numerical simulations confirmed the theoretical analysis. The analysis of the two-parameter family proposed in this paper for the 2-dof vibro-impact system developed the results of one-parameter family by other authors. It shows that there exists complicated and interesting dynamic behavior of the vibro-impact system near order 4 resonant point, which matches the study in the Krauskopf papers [18,19]. The tori bifurcation and the route of quasi-periodic impacts to chaos are also reported briefly. It seems to us that our method could well be applied to investigate bifurcations of periodic motions in different kinds of vibrating systems with or without impacts.

Acknowledgements

This work is supported by the National Science Foundation of China (10472096), Specialized Research Fund for the Doctoral Program of Higher Education of China (20010613001) and 'Qing Lan' Talent Engineering Funds by Lanzhou Jiaotong University.

References

[1] P.J. Holmes, The dynamics of repeated impacts with a sinusoidally vibrating table, *Journal of Sound and Vibration* 84 (2) (1982) 173–189.

[2] J.M.T. Thompson, Chaos after period-doubling bifurcations in the resonance of an impact oscillator, *Physics Letters* 91A (1983) 5–8.
[3] S.W. Shaw, P.J. Homles, Periodically forced linear oscillator with impacts: chaos and long-period motions, *Physical Review Letters* 51 (8) (1983) 623–626.
[4] G.S. Whiston, Singularities in vibro-impact dynamics, *Journal of Sound and Vibration* 152 (3) (1992) 427–460.
[5] A.P. Ivanov, Stabilization of an impact oscillator near grazing incidence owing to resonance, *Journal of Sound and Vibration* 162 (3) (1993) 562–565.
[6] A.B. Nordmark, Non-periodic motion caused by grazing incidence in an impact oscillator, *Journal of Sound and Vibration* 145 (2) (1991) 279–297.
[7] G.W. Luo, J.H. Xie, Hopf bifurcations of a two-degree-of-freedom vibro-impact system, *Journal of Sound and Vibration* 213 (3) (1998) 391–480.
[8] J.H. Xie, Codimension two bifurcations and Hopf bifurcations of an impacting vibrating system, *Applied Mathematics and Mechanics* 17 (1) (1996) 65–75.
[9] G.L. Wen, Codimension-2 Hopf bifurcation of a two-degree-of-freedom vibro-impact system, *Journal of Sound and Vibration* 242 (3) (2001) 475–485.
[10] G.L. Wen, J.H. Xie, Period-doubling bifurcation and non-typical route to chaos of a two-degree-of-freedom vibro-impact system, *Journal of Applied Mechanics* 68 (4) (2001) 670–674.
[11] G. Iooss, Bifurcation of maps and applications, *Mathematics Studies*, vol. 36, North-Holland, Amsterdam, 1979.
[12] A. Chenciner, G. Iooss, Bifurcation de torus invariant, *Archive for Rational Mechanics and Analysis* 69 (1979) 109–198.
[13] Y.H. Wan, Bifurcation into invariant tori at points of resonance, *Archive for Rational Mechanics and Analysis* 68 (1978) 343–357.
[14] V.I. Arnold, *Geometrical Methods in the Theory of Ordinary Differential Equations*, Springer, Berlin, 1983.
[15] V.I. Arnold, Loss of stability of self-oscillations close to resonance and versal deformations of equivariant vector fields, *Funktsional nvi Analiz i ego Prilozheniya* 11 (2) (1977) 1–10.
[16] G.W. Luo, J.H. Xie, Hopf bifurcations and chaos of a two-degree-of-freedom vibro-impact system in two strong resonance cases, *International Journal of Non-linear Mechanics* 37 (1) (2002) 19–34.
[17] F.S. Berezovskaia, A.I. Khibnik, On the bifurcations of seperatrices in the problem of stability loss of auto-oscillations near 1:4 resonance, *Prikladnaya Matematika Mekhanika* 44 (1980) 663–667.
[18] B. Krauskopf, Bifurcation sequences at 1:4 resonance: an inventory, *Nonlinearity* 7 (1994) 1073–1091.
[19] B. Krauskopf, The bifurcation set for the 1:4 resonance problem, *Experimental Mathematics* 3 (2) (1995) 107–128.
[20] J. Carr, *Applications of Center Manifold Theory*, Applied Mathematical Sciences, vol. 35, Springer, Berlin, 1981, pp. 33–36.